CrystEngComm

RSC Publishing

PAPER

View Article Online
View Journal | View Issue

Cite this: *CrystEngComm*, 2013, **15**, 7583

Assembly of multinuclear Ag complexes and Keggin polyoxometalates adjusted by organic ligands: syntheses, structures and luminescence†

Zhen-yu Shi,[ab] Jun Peng,*[a] Yang-guang Li,*[a] Zhe-yu Zhang,[a] Xia Yu,[a] Kundawlet Alimaje[a] and Xiang Wang[a]

Received 4th July 2013,
Accepted 18th July 2013

DOI: 10.1039/c3ce41312h

www.rsc.org/crystengcomm

Two unusual α-Keggin-based compounds with multinuclear silver clusters, $\{[Ag_7(H_2biim)_5][PW_{11}O_{39}]\}\cdot Cl\cdot H_3O$ (**1**) and $\{[Ag_2(H_2biim)_2][Ag(phnz)](PW_{12}O_{40})\}\cdot H_2O$ (**2**) (H_2biim = 2,2′-biimidazole, phnz = phenazine), have been hydrothermally synthesized and structurally characterized by elemental analyses, IR spectra, thermogravimetric analysis and X-ray crystallography. Compound **1** displays a 2D network featuring dimerized monolacunary Keggin anions $\{PW_{11}O_{39}\}_2$ which are connected together through pentanuclear silver clusters. Interestingly, besides $\{Ag_5\}^{5+}$ clusters, there are another kinds of argentophilic $\{Ag_4\}^{4+}$ clusters coexisting in compound **1**. Compound **2** consists of four subunits: 1D cationic chains $[Ag(phnz)]^+$, dinuclear silver-H_2biim units $[Ag_2(H_2biim)_2]^{2+}$, discrete polyanions $\{PW_{12}O_{40}\}^{3-}$ and water molecules, which are further joined by hydrogen bonds to form a 3D supramolecular structure. The differences in the structures of compounds **1** and **2** indicate that the introduction of the secondary organic ligand plays a key role in determining the final structure. The electrochemical, electrocatalytic behaviors and luminescent properties of compounds **1** and **2** have also been investigated.

Introduction

The polyoxometalates (POMs) are a large family of anionic transition metal oxide clusters with a rich molecular structural variety with different sizes, shapes and nuclearities.[1] These properties make POMs ideal candidates for constructing functional materials with potential applications in a wide range of fields including catalysis, electrochemistry, photochromism, magnetism and drug delivery.[2] With the aim of synthesizing POM-based functional materials with a unique architecture and desirable properties, much work has been focused on the decoration of POMs with transition metals and/or organic species.[3] Recently, POM-based compounds decorated by multisilver clusters have evoked an immense amount of interest not only because of the larger sizes and multiple coordination sites of the multisilver clusters, but also because of their unusual properties that are different from those of mononuclear silver compounds.[4] The silver ion has been utilized to functionalize multimetal POMs owing to the following reasons: (i) its high affinity to N and O donors, (ii) its flexible coordination numbers varying greatly from two to nine, (iii) argentophilic Ag···Ag interactions, and (iv) the synergistic effects between multisilver clusters and POMs which may enhance the efficiency of catalysts.[5] Furthermore, to encourage the formation of the Ag···Ag interactions, it is vital to choose proper solvents or multidentate organic ligands as diverse as triazoles and tetrazoles which are capable of interconnecting metal centers. To date, some multisilver POMs have been constructed.[5,6] For example, in 2012, Mizuno's group synthesized a discrete octahedrally shaped $[Ag_6]^{4+}$ cluster which was encapsulated within two $[\gamma\text{-}H_2SiW_{10}O_{36}]^{6-}$ subunits.[6a] In the same year, they also prepared a diamond-shaped $[Ag_4]^{4+}$ cluster encapsulated by silicotungstates.[5] Cronin *et al.* obtained a truly porous 3D framework $[Ag(CH_3CN)_4] \subset \{[Ag(CH_3CN)_2]_4[H_3W_{12}O_{40}]\}$ which consisted of $[Ag_2]^{2+}$ clusters and $[H_3W_{12}O_{40}]^{5-}$ anions.[6c] Wang *et al.* synthesized two novel one-dimensional Keggin-based coordination polymers with $\{Ag_3\}^{3+}/\{Ag_4\}^{4+}$ clusters.[4a] Among these reported compounds, silver clusters present di-nuclear, tri-nuclear, tetra-nuclear or infinite structures, whereas POMs mainly focus on saturated Keggin and $[\gamma\text{-}H_2SiW_{10}O_{36}]^{6-}$ anions. To the best of our knowledge, silver clusters encapsulated by monolacunary Keggin anions have never been described.

As is known to all, the properties and potential functionalities of multisilver POMs are related to the structural and chemical features of the organic ligands. Hence, the choice of

[a]*Key Laboratory of Polyoxometalate Science of Ministry of Education, Department of Chemistry, Northeast Normal University, Changchun, Jilin, 130024, P. R. China. E-mail: jpeng@nenu.edu.cn; liyg658@nenu.edu.cn; Fax: +86-431-85099372; Tel: +86-431-82684009*

[b]*Xingyi Normal College for Nationalities, Xingyi, Guizhou, 562400, P. R. China*

† Electronic supplementary information (ESI) available. CCDC numbers 912980 and 912981. For ESI and crystallographic data in CIF or other electronic format see DOI: 10.1039/c3ce41312h

ligands is crucial. Among the numerous multidentate ligands, H_2biim (H_2biim = 2,2′-biimidazole) looks particularly attractive. Firstly, the two imidazole rings in H_2biim can distort freely to meet the different coordination modes. Secondly, the proper distances between two N donors benefit the formation of Ag···Ag interactions. We have been particularly interested in the modular assembly of multisilver POMs based on H_2biim.[4c] Meanwhile, during the preparation of multisilver POMs, we have focused on the study of factors influencing the size of the silver clusters. Toward this end, we introduced a secondary ligand phnz (phnz = phenazine) into the Ag/POM/H_2biim system, in hopes of getting more information about whether the secondary ligands influence the size of the silver clusters. As far as we know, such work has not been reported in the chemistry of multimetal POMs. Herein, we report two novel compounds, $\{[Ag_7(H_2biim)_5][PW_{11}O_{39}]\}\cdot Cl\cdot H_3O$ (**1**) and $\{[Ag_2(H_2biim)_2][Ag(phnz)](PW_{12}O_{40})\}\cdot H_2O$ (**2**). Compound **1** shows a 2D network featuring dimerized monolacunary Keggin anions $\{PW_{11}O_{39}\}_2$ which are connected together through pentanuclear silver clusters. Compound **2** is a 3D supramolecular structure composed of 1D cationic chains $[Ag(phnz)]^+$, dinuclear silver–H_2biim units $[Ag_2(H_2biim)_2]^{2+}$, discrete polyanions $\{PW_{12}O_{40}\}^{3-}$ and water molecules. The difference in the structures of compounds **1** and **2** indicates that the introduction of the secondary organic ligand plays a key role in determining the final structure. To the best of our knowledge, compound **1** represents the first $\{Ag_5\}^{5+}$ cluster encapsulated between two monolacunary Keggin anions.

Experimental section

Material and physical measurements

All reagents and solvents for the syntheses were purchased from commercial sources and used without further purification. Elemental analyses (C, H and N) were performed on a Perkin-Elmer 2400 CHN Elemental Analyzer. Ag was determined by a Leaman inductively coupled plasma (ICP) spectrometer. Scanning electron microscopy energy-dispersive spectrometry (SEM-EDS) was taken with an XL30 field emission environmental scanning electron microscope to identify the presence of the Cl atom. IR spectra were obtained on Alpha Centaurt FT-IR spectrometer with a KBr pellet in the 400–4000 cm^{-1} region. The TG analyses were performed on a Perkin-Elmer TGA7 instrument in flowing N_2 with a heating rate of 10 °C min^{-1}. The solid state photoluminescent spectra were recorded on an FLSP920 Edinburgh Fluorescence Spectrometer at room temperature. The XPRD patterns were obtained with a Rigaku D/Max 2500V PC diffractometer with Cu Kα radiation, with a scanning rate of 4° s^{-1}, 2θ ranging from 5–50°. Cyclic voltammograms were obtained with a CHI 660 electrochemical workstation at room temperature. A platinum gauze was used as the counter electrode and Ag/AgCl was used as the reference electrode. A chemically bulk-modified carbon paste electrode (CPE) was used as the working electrode.

The synthesis of $\{[Ag_7(H_2biim)_5][PW_{11}O_{39}]\}\cdot Cl\cdot H_3O$ (1). A reaction mixture of $AgNO_3$ (0.051 g, 0.3 mmol), $H_3[PW_{12}O_{40}]\cdot 12H_2O$ (0.310 g, 0.1 mmol) and H_2biim (0.065 g, 0.5 mmol) was dissolved in 8 mL of distilled water at room temperature. The resulting suspension was stirred for 0.5 h and the pH value of the mixture solution was carefully adjusted to about 2.3 with 1 mol L^{-1} NaOH and HCl. Then the mixture was sealed in an 18 mL Teflon-lined stainless steel vessel under autogeneous pressure and heated at 160 °C for five days. Red block crystals were isolated and washed with distilled water. Yield: 0.256 g (56% based on tungsten). Elemental analysis found: C, 8.48; H, 0.78; N, 6.56; Ag, 18.09%. Calc. for compound **1**, $C_{60}H_{70}Ag_{14.4}W_{22}Na_{1.6}N_{40}O_{84}P_2$, (8391.93): C, 8.67; H, 0.80; N, 6.74; Ag, 18.16%.

The synthesis of $\{[Ag_2(H_2biim)_2][Ag(phnz)](PW_{12}O_{40})\}\cdot H_2O$ (2). The preparation of compound **2** was similar to that of **1**, except that phnz (0.090 g, 0.5 mmol) was added. Red block crystals were isolated and washed with distilled water. Yield: 0.154 g (42% based on tungsten). Elemental analysis found: C, 7.79; H, 0.50; N, 3.73; Ag, 8.74%. Calc. for compound **2** $C_{24}H_{20}Ag_3W_{12}N_{10}O_{41}P$, (3665.12): C, 7.86; H, 0.55; N, 3.82; Ag, 8.83%.

The preparation of 1-CPE and 2-CPE. 90 mg graphite powder and 10 mg **1** or **2** were mixed and ground together by agate mortar and pestle to achieve an even, dry mixture. To the mixture 0.12 ml nujol was added and stirred with a glass rod. Then the homogenized mixture was packed into a 1.2 mm inner diameter glass tube, and the surface was wiped with paper. Electrical contact was established with the copper rod through the back of the electrode.

X-ray crystallography

The crystal data for compounds **1** and **2** were collected on an Oxford Diffraction Gemini R Ultra diffractometer, with Mo K monochromated radiation (λ = 0.71073 Å). All structures were solved by directed methods and refined by full-matrix least-squares on F^2 using the SHELXTL crystallographic software package.[7] The positions of the hydrogen atoms on the carbon atoms were calculated theoretically. All hydrogen atoms attached to water molecules were not located.

A summary of the crystallographic data and structural determination for them is provided in Table 1. Selected bond lengths and angles of the two compounds are listed in Table S1, ESI.† The crystallographic data for the structures reported in this paper have been deposited in the Cambridge Crystallographic Data Center with CCDC numbers 912981 for **1** and 912980 for **2**.

Results and discussion

Description of the crystal structures

The crystal structure of $\{[Ag_7(H_2biim)_5][PW_{11}O_{39}]\}\cdot Cl\cdot H_3O$ 1. Compound **1** crystallizes in the triclinic space group $P\bar{1}$. The fundamental building unit of **1** contains one crystallographically independent $PW_{11}O_{39}^{7-}$ (labelled as PW_{11}), seven Ag(I) cations, five H_2biim ligands, one chloride ion and one protonated water molecule. The chloride ions in compound

Table 1 Crystal data collections and structure refinements for **1** and **2**

	1	**2**
Formula	$C_{30}H_{33}Ag_7ClN_{20}O_{40}PW_{11}$	$C_{24}H_{20}Ag_3W_{12}N_{10}O_{41}P$
M	4157.44	3665.12
T/K	296(2)	293(2)
Crystal system	Triclinic	Tetragonal
Space group	$P\bar{1}$	$P4_2/n$
a/Å	12.7243(13)	20.222(5)
b/Å	14.7895(15)	20.222(5)
c/Å	19.0990(19)	14.199(5)
α/°	106.5030(10)	90.00
β/°	95.4970(10)	90.00
γ/°	99.0920(10)	90.00
V/Å^3	3365.0(6)	5806(3)
Z	2	4
D_c/Mg m^{-3}	4.094	4.213
μ/mm^{-1}	20.865	24.782
F(000)	3678	6464
θ range/°	1.46–25.00	3.04–25.00
Reflections collected	16 830	21 347
Independent reflections (R_{int})	11 668(0.0269)	5095(0.0669)
GOF	1.078	1.134
Final $R^{a,b}$ indices [$I > 2\sigma(I)$]	R_1 = 0.0553, wR_2 = 0.1492	R_1 = 0.0531, wR_2 = 0.1004
R indices (all data)	R_1 = 0.0761, wR_2 = 0.1601	R_1 = 0.0845, wR_2 = 0.1125

^{a} $R_1 = \Sigma||F_o| - |F_c||/\Sigma|F|$. ^{b} w$R_2 = |\Sigma w(|F_o|^2 - |F_c|^2)^2/\Sigma|w(F)^2|^{1/2}$.

1 function as counter ions. In compound **1**, it is interesting that PW_{11} is formed from the saturated Keggin cluster PW_{12} under hydrothermal conditions and one Ag(I) cation physically occupies the vacant position of PW_{11} to generate an anionic $[AgPW_{11}O_{39}]^{6-}$ unit. The $[AgPW_{11}O_{39}]^{6-}$ cluster is structurally identical with that in the compound first reported by Nogueira.[8] With the exception of this example, no other compounds built from $[AgPW_{11}O_{39}]^{6-}$ clusters have been found so far. In $AgPW_{11}$, the central P atom is surrounded by four oxygen atoms (O1, O2, O3 and O19). The P–O average distance is in the usual region of 1.544(1) Å and the O–P–O bond angle is in the range of 108.3(7)–111.5(7)°. The distances of the W–O bonds can be divided into three groups: W–O_a, 2.339(1)–2.455(1) Å, W–O_b, 1.752(1)–2.083(1) Å, W–O_t, 1.695(1)–1.751(5) Å. The valence sum calculations show that all of the tungsten atoms are in the 6+ oxidation state.[9]

A remarkable structural feature of compound **1** is the presence of two kinds of multisilver clusters: $\{Ag_5\}^{5+}$ and $\{Ag_4\}^{4+}$. $\{Ag_5\}^{5+}$ is encapsulated by two neighboring monolacunary Keggin anions PW_{11} (Fig. 1a). In the $\{Ag_5\}^{5+}$ cluster, three crystallographically independent Ag(I) ions are Ag5, Ag6 and Ag7. Ag5 displays a distorted octahedral geometry, defined by six terminal oxygen atoms: four oxygen atoms O4, O5, O28 and O38 from one PW_{11}, and two oxygen atoms O4# and O28# from another PW_{11}. The Ag–O bond distances range from 2.345(1) Å to 2.502(2) Å. Ag6 with a 50% occupancy, adopts a Y-shaped geometry, coordinated by one nitrogen atom N23 (Ag6–N23 = 1.84(5) Å) from one H_2biim molecule, and two terminal oxygen atoms O4 and O38 from the same PW_{11} (Ag6–O4 = 2.462(13) Å, Ag6–O38 = 2.384(14) Å). Ag7 is disordered and adopts a Y-shaped trigonal geometry, coordinated by two terminal oxygen atoms O30, O32 and O38 from three AgW_{11} (Ag7–O30 = 2.247(14) Å, Ag7–O32 = 2.401(17), Ag7–O38 = 2.644(2) Å).

The adjacent six Ag(I) ions are aggregated by a pair of PW_{11} polyanions to generate a pentanulcear cluster. In the $\{Ag_5\}^{5+}$ cluster, the intermetallic distances of Ag5–Ag6, Ag5–Ag5#3 and Ag7–Ag6 are 3.247(4) Å, 2.864(3) Å and 2.892(8) Å, respectively, which are shorter than twice the van der Waals radius of the silver atom (3.44 Å). This suggests the existence of argentophilic interactions in the $\{Ag_5\}^{5+}$ cluster. $\{Ag_5\}^{5+}$ joins two adjacent PW_{11} anions together to form an unprecedented dimerized $[PW_{11}O_{39}Ag_5]_2^{4-}$ polyanion which functions as a tetradentate ligand to link four Ag8 ions. To date, POMs with

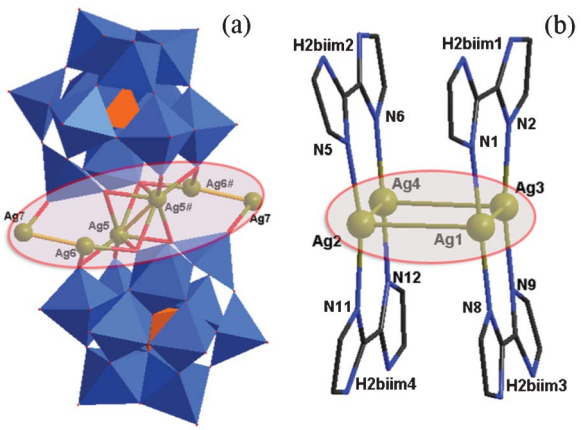

Fig. 1 (a) The polyhedral and ball-and-stick representation of the $[PW_{11}O_{39}Ag_5]_2^{4-}$ polyanion; (b) the view of the $\{Ag_4\}^{4+}$ cluster in **1**. Color codes: yellow, Ag; blue, N; black, C.

$\{Ag_5\}^{5+}$ clusters encapsulated between two monolacunary Keggin anions have not been reported.

As shown in Fig. 1b, the $\{Ag_4\}^{4+}$ cluster is approximately square. In the $\{Ag_4\}^{4+}$ cluster, there are four crystallographically unique Ag(I) ions, namely, Ag1, Ag2, Ag3 and Ag4. Ag1 presents a linear geometry with one nitrogen atom N1 (Ag1–N1 = 2.117(1) Å) from a H_2biim1 ligand, and one nitrogen atom N8 (Ag1–N8 = 2.105(2) Å) from a H_2biim3 ligand. Ag2 is surrounded by one nitrogen atom N5 from a H_2biim2 ligand (Ag2–N5 = 2.098(2) Å) and one nitrogen atom N11 from a H_2biim4 ligand (Ag2–N11 = 2.135(2) Å) in a linear geometry. Ag3 is three-coordinated in a "Y-shaped" geometry, coordinated by one disordered chloride ion and two nitrogen atoms N2 and N9 which are from the H_2biim2 and H_2biim3 ligands, respectively (Ag3–N2 = 2.107(2) Å, Ag3–N9 = 2.12(2) Å). Ag4 exhibits a linear coordination environment formed by one nitrogen atom, N6, from H_2biim2 (Ag4–N6 = 2.097(2) Å) and by one N atom N12 from one H_2biim4 (Ag4–N12 = 2.108(1) Å). The N6–Ag4–N12 bond angle is 166.7(1)°. In the $\{Ag_4\}^{4+}$ cluster, the distances of Ag1–Ag2, Ag2–Ag4, Ag4–Ag3 and Ag3–Ag1 are 3.184(4) Å, 2.790(3) Å, 3.233(5) Å and 2.769(3) Å, respectively, suggesting Ag(I)···Ag(I) interactions. The Ag4–Ag2–Ag1 and Ag2–Ag1–Ag3 bond angles are 100.3(0)° and 80.5(9)°, respectively, showing that the shape of the $\{Ag_4\}^{4+}$ cluster is close to a square. The $\{Ag_4\}^{4+}$ clusters in compound **1** act as counter-cations.

The Ag8(I) ion is four-coordinated, formed by one chloride ion, one N atom (N19) from one H_2biim5 (Ag8–N19 = 2.333(1) Å) and two oxygen atoms (O16 and O29) from two PW_{11} anions (Ag8–O16 = 2.369(2) Å, Ag8–O29 = 2.513(2) Å). All of the H_2biim ligands in **1** act as bidentate bridging linkers. Two neighboring Ag8 ions are joined through one H_2biim ligand to generate a complex fragment $[Ag_2(H_2biim)]^{2+}$, which can be considered as four-connected nodes.

In compound **1**, neighboring dimerized $[PW_{11}O_{39}Ag_5]_2^{4-}$ polyanions are fused together *via* Ag7 ions, leading to a 1D chain $\{PW_{11}O_{39}Ag_5\}_n$ (Fig. 2). The Ag8 ions further link the 1D chains $\{PW_{11}O_{39}Ag_5\}_n$ together through oxygen atoms (O16 and O29) along the *c* axis to result in a 2D layer (Fig. 3).

The crystal structure of $\{[Ag_2(H_2biim)_2][Ag(phnz)](PW_{12}O_{40})\}\cdot H_2O$ 2. Single-crystal X-ray analysis shows that the structure of compound **2** contains four kinds of subunits, that is, 1D Ag–phnz chains, dinuclear silver–H_2biim units, discrete polyanions $\{PW_{12}O_{40}\}$ (labelled as PW_{12}) and water molecules, respectively (see Fig. 4). In compound **2**, the PW_{12} anion is the classical α-Keggin-type. The central P atom in each polyanion is located at the inversion center, which results in a disordered PO4

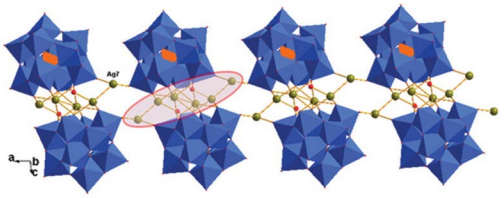

Fig. 2 The view of the 1D chain constructed from $[PW_{11}O_{39}Ag_5]_2^{4-}$ anions in **1**.

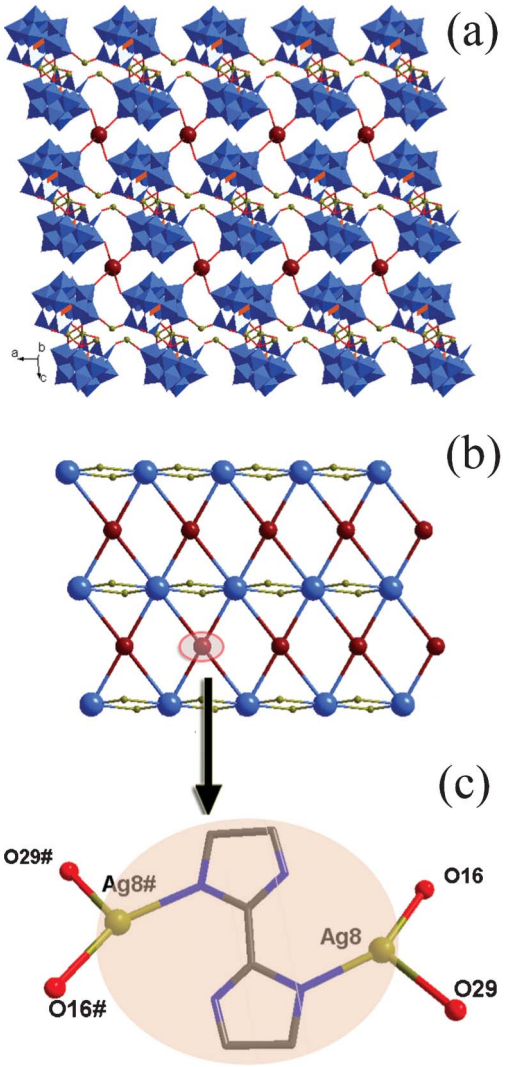

Fig. 3 (a) The view of the 2D structure of **1** constructed from 1D chains $\{PW_{11}O_{39}Ag_5\}_n$ and Ag8 ions; (b) the schematic view of the 2D network; (c) the view of the four-connected nodes of $[Ag_2(H_2biim)]^{2+}$.

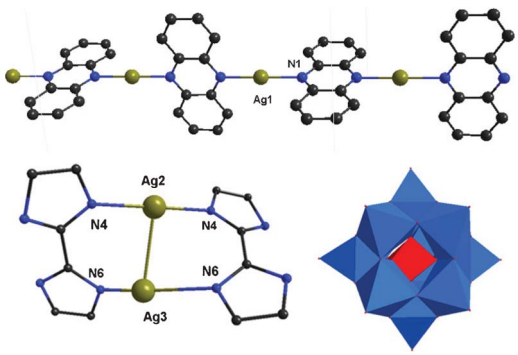

Fig. 4 The view of three subunits in compound **2**: 1D Ag–phnz chains, dinuclear silver–H_2biim units and discrete polyanions $\{PW_{12}O_{40}\}$.

tetrahedron, that is, the central P atom is surrounded by a cube of eight oxygen atoms, with each oxygen site half-occupied.

In the dinuclear cluster $[Ag_2(H_2biim)_2]^{2+}$, Ag2 is coordinated by two nitrogen atoms (N4) from two H_2biim ligands to complete a linear coordination geometry (Ag2–N4 = 2.14(5) Å). Similarly, Ag3 is also two-coordinated with the Ag3–N6 distance of 2.47(6) Å. H_2biim, acting as a bidentate bridging linker, connects the adjacent Ag(I) ions to generate a dinuclear cluster. The imidazole rings in each H_2biim molecule are not in the same plane. The twisted angle is *ca.* 28.74°. The close Ag(I)···Ag(I) distance supported by H_2biim is *ca.* 2.82(4) Å, which is obviously shorter than the van der Waals radii of the two silver atoms (3.44 Å) and indicates strong Ag(I)–Ag(I) interactions.

It is interesting that a 1D Ag–phnz chain exists. In the Ag–phnz chain, Ag1 displays a linear coordination geometry, coordinated by two nitrogen atoms from two phnz ligands (Ag1–N1 = 2.16(3) Å, Ag1–N2 = 2.16(6) Å).

These four subunits are joined together through hydrogen bonding interactions (O9···N2 = 3.06 Å, Ow1···N3 = 2.92 Å), thus resulting in a 3D supramolecular array (Fig. S1, ESI†).

The influence of the secondary ligand phnz on the structures of compounds 1 and 2

Both compounds **1** and **2** were directly isolated at a high temperature under hydrothermal conditions. The only difference deals with the introduction of the secondary bridging ligand phnz ligand to the reaction system of compound **2**, which leads to the structural transformation. When competing with H_2biim, the polycyclic aromatic ligand phnz has bigger steric hindrance, which induces the Ag(I) ions to form compounds in a lower coordination number and transfers the structure from a 2D network with $\{Ag_6\}^{6+}/\{Ag_4\}^{4+}$ clusters to a 1D chain with $\{Ag_2\}^{2+}$ clusters.

FT-IR spectra, TG and XRD analyses

The IR spectra of compounds **1** and **2** are shown in Fig. S2 (ESI†). The characteristic bands at 1079, 946, 837 and 760 cm^{-1} for **1** and 1079, 970, 887 and 768 for **2** are attributed to the (P–O), (W–Ot) and (W–Ob–W) vibrations of the PW12 anions, respectively. The peaks at 1624, 1541 and 1414 cm^{-1} in compound **1** and 1624, 1541, 1465 and 1440 cm^{-1} in compound **2**, are characteristic of the organic ligands.

The thermogravimetric analyses (TGA) also support the chemical compositions of compounds **1** and **2** (Fig. S3, ESI†). Both curves show two steps of weight loss processes. The TGA curve for **1** shows an initial weight loss of 0.52% (calc. 0.43%) from 70 °C to 160 °C corresponding to the removal of lattice water molecules, while the weight loss at 160–690 °C, 17.11% (calc. 16.12%) is ascribed to the decomposition of the H_2biim ligands. In compound **2**, the first weight loss of 0.62% (calc. 0.49%) below 247 °C is due to the loss of lattice water molecules, while the second weight loss of 12.03% (calc. 12.22%) in the range of 247–620 °C is ascribed to the decomposition of the H_2biim and phnz ligands.

The PXRD patterns of compounds **1** and **2** confirm the good phase purity since the simulated and experimental data are similar (Fig. S4, ESI†).

Photoluminescent properties

POM-based hybrids with Ag(I) ions and conjugated ligands are of great interest owing to their the excellent luminescence performance. The luminescence studies of compounds **1** and **2** and the ligands H_2biim and phnz are explored in the solid state at room temperature. The emission bands are centered at about 444 nm (λ_{ex} = 370 nm) for H_2biim, and 480 and 512 nm (λ_{ex} = 445 nm) for phnz, which may be attributed to the ligand-centered π*–π electronic transitions (Fig. S5, ESI†). Comparably, compound **1** displays the similar emission band at *ca.* 415 nm when excitation occurs at 336 nm. Compound **2** exhibits an intense photoluminescence with an emission maximum occurring at 493 nm upon excitation at 370 nm (Fig. S6, ESI†). Compared with the free organic ligands, the emission intensity decreases, which may be due to the hydrogen bonding interactions between the organic ligands and the guest water molecule.

Cyclic voltammetry

The electrochemical properties of **1**- and **2**-CPE have been investigated in detail in a 1 M H_2SO_4 + 0.2 M Na_2SO_4 aqueous solution. In the potential range from −700 to +400 mV, there are two pairs of reversible redox peaks (I–I′ and II–II′) for compound **1**, which could be assigned to the redox process of $W^{VI/V}$. The mean peak potentials $E_{1/2} = (E_{cp} + E_{ap})/2$ are −349 and −546 mV, respectively. For compound **2**, three pairs of reversible redox peaks (I–I′, II–II′ and III–III′) could be found and the peak potentials $E_{1/2} = (E_{cp} + E_{ap})/2$ are +150, −156 and −384 mV which could be ascribed to the redox process of $Ag^{I/0}$ and $W^{VI/V}$ (Fig. 5). At the same time, with the scan rate varying from 20 to 180 mV s^{-1}, the peak potentials change gradually: the cathodic peak potentials shift toward the negative direction and the corresponding anodic peak potentials shift toward the positive direction.

Fig. 6 shows the electrocatalytic behavior of **1**- and **2**-CPE in 1 M H_2SO_4 + 0.2 M Na_2SO_4 + $NaNO_2$. It can be clearly seen that when the concentration of nitrite increases (from 0 to 12 mM), the reduction peak currents gradually increase while the corresponding oxidation markedly decreases. This fact displays the good electrocatalytic activity of **1**- and **2**-CPE toward the reduction of nitrite.

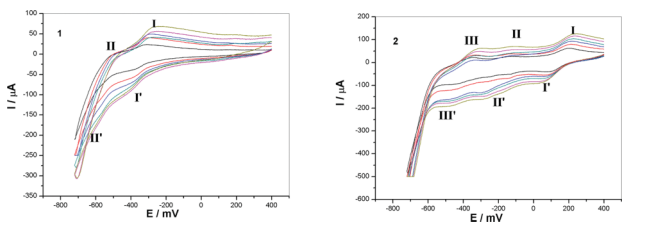

Fig. 5 Cyclic voltammograms of **1**- and **2**-CPE in a 1 M H_2SO_4 + 0.2 M Na_2SO_4 solution at different scan rates (from inner to outer: 20, 50, 100, 120, 150 and 180 mV s^{-1}).

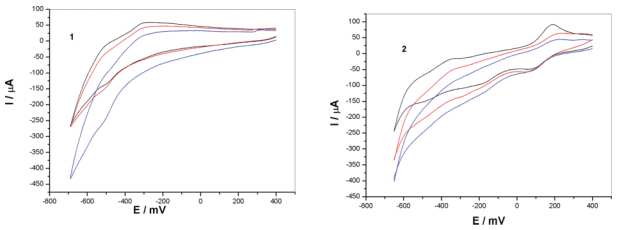

Fig. 6 Cyclic voltammograms of **1**- and **2**-CPE in a 1 M H_2SO_4 + 0.2 M Na_2SO_4 solution containing 0, 6 and 12 mM $NaNO_2$ (scan rates: 100 mV s^{-1}).

Conclusions

In this paper, by introducing the polycyclic aromatic ligand phnz to the Ag/POM/H_2biim system, two unusual compounds with argentophilic $\{Ag_5\}^{5+}$–$\{Ag_4\}^{4+}$/$\{Ag_2\}^{2+}$ clusters have been hydrothermally synthesized. Compound **1** represents the first example of a POM with $\{Ag6\}^{6+}$ clusters encapsulated between two monolacunary Keggin anions. Compound **2** is a 1D chain with $\{Ag_2\}^{2+}$ clusters. The differences in the structures of compounds **1** and **2** indicate that the secondary organic ligands make the difference in determining the size of the multisilver cluster in the final structure. Other factors which may influence the size of multisilver clusters in POMs are under investigation.

Acknowledgements

This work was financially supported by the National Natural Science Foundation of China (No. 21071029) and the Science and Technology Foundation of Guizhou Province (20132278). We thank Professor Yanhui Chen for helping crystallographic structural analysis.

Notes and references

1 (*a*) D. L. Long, E. Burkholder and L. Cronin, *Chem. Soc. Rev.*, 2007, **36**, 105; (*b*) A. Dolbecq, E. Dumas, C. R. Mayer and P. Mialane, *Chem. Rev.*, 2010, **110**, 6009.

2 (*a*) C. Y. Sun, S. X. Liu, D. D. Liang, K. Z. Shao, Y. H. Ren and Z. M. Su, *J. Am. Chem. Soc.*, 2009, **131**, 1883; (*b*) K. Nomiya, H. Yanagibayashi, C. Nozaki, K. Kondoh, E. Hiramatsu and Y. Shimizu, *J. Mol. Catal. A: Chem.*, 1996, **114**, 181; (*c*) G. Bernardini, C. Zhao, A. G. Wedd and A. M. Bond, *Inorg. Chem.*, 2011, **50**, 5899; (*d*) Y. F. Wang and I. A. Weinstock, *Chem. Soc. Rev.*, 2012, **41**, 7479.

3 (*a*) J. X. Lin, J. Lü, H. X. Yang and R. Cao, *Cryst. Growth Des.*, 2010, **10**, 1966; (*b*) H. Fu, C. Qin, Y. Lu, Z. M. Zhang, Y. G. Li, Z. M. Su, W. L. Li and E. B. Wang, *Angew. Chem., Int. Ed.*, 2012, **51**, 7985; (*c*) J. Q. Sha, J. Peng, Y. Zhang, H. J. Pang, A. X. Tian, P. P. Zhang and H. Liu, *Cryst. Growth Des.*, 2009, **9**, 1708; (*d*) Y. Z. Gao, Y. Q. Xu, Z. G. Han, C. H. Li, F. Y. Cui, Y. N. Chi and C. W. Hu, *J. Solid State Chem.*, 2010, **183**, 1000; (*e*) X. L. Wang, Y. F. Wang, G. C. Liu, A. X. Tian, J. W. Zhang and H. Y. Lin, *Dalton Trans.*, 2011, **40**, 9299; (*f*) J. P. Wang, J. Du and J. Y. Niu, *CrystEngComm*, 2008, **10**, 972; (*g*) J. W. Zhao, H. P. Jia, J. Zhang, S. T. Zheng and G. Y. Yang, *Chem.–Eur. J.*, 2007, **13**, 10030; (*h*) E. Burkholder and J. Zubieta, *Solid State Sci.*, 2004, **6**, 1421; (*i*) W. Q. Kan, J. Yang, Y. Y. Liu and J. F. Ma, *Inorg. Chem.*, 2012, **51**, 11266; (*j*) R. N. Devi and J. Zubieta, *Inorg. Chim. Acta*, 2003, **343**, 313.

4 (*a*) L. M. Dai, W. S. You, E. B. Wang, S. X. Wu, Z. M. Su, Q. H. Du, Y. Zhao and Y. Fang, *Cryst. Growth Des.*, 2009, **9**, 2110; (*b*) X. Wang, J. Peng, K. Alimajea and Z. Y. Shi, *CrystEngComm*, 2012, **14**, 8509; (*c*) P. P. Zhang, J. Peng, H. J. Pang, J. Q. Sha, M. Zhu, D. D. Wang and M. G. Liu, *CrystEngComm*, 2011, **13**, 3832; (*d*) Q. G. Zhai, X. Y. Wu, S. M. Chen, Z. G. Zhao and C. Z. Lu, *Inorg. Chem.*, 2007, **46**, 5046; (*e*) F. Gruber and M. Jansen, *Inorg. Chim. Acta*, 2010, **363**, 4282; (*f*) X. L. Wang, H. L. Hu and A. X. Tian, *Cryst. Growth Des.*, 2010, **10**, 4786; (*g*) X. L. Wang, D. Zhao, A. X. Tian and J. Ying, *CrystEngComm*, 2013, **15**, 4516.

5 Y. Kikukawa, Y. Kuroda, K. Yamaguchi and N. Mizuno, *Angew. Chem., Int. Ed.*, 2012, **51**, 2434.

6 (*a*) Y. Kikukawa, Y. Kuroda, K. Suzuki, M. Hibino, K. Yamaguchi and N. Mizuno, *Chem. Commun.*, 2013, **49**, 376; (*b*) R. Villanneau, A. Proust, F. Robert and P. Gouzerh, *Chem. Commun.*, 1998, 1491; (*c*) C. Streb, C. Ritchie, D. L. Long, P. Kögerler and L. Cronin, *Angew. Chem., Int. Ed.*, 2007, **46**, 7579; (*d*) G. G. Gao, P. S. Cheng and T. C. W. Mak, *J. Am. Chem. Soc.*, 2009, **131**, 18257; (*e*) H. Abbas, C. Streb, A. L. Pickering, A. R. Neil, D. L. Long and L. Cronin, *Cryst. Growth Des.*, 2008, **8**, 635; (*f*) F. Gruber and M. Jansen, *Angew. Chem., Int. Ed.*, 2010, **49**, 4924.

7 (*a*) G. M. Sheldrick, *SHELX-97, Program for Crystal Structure Refinement*, University of Göttingen, Germany, 1997; (*b*) G. M. Sheldrick, *SHELXL-97, Program for Crystal Structure Solution*, University of Göttingen, Germany, 1997.

8 H. I. S. Nogueira, F. A. Almeida Paz, P. A. F. Teixeiraa and J. Klinowskib, *Chem. Commun.*, 2006, 2953.

9 I. D. Brown and D. Altermatt, *Acta Crystallogr., Sect. B: Struct. Sci.*, 1985, **41**, 244.

